J|A|C|S
ARTICLES
Published on Web 06/19/2002

Synthesis, Characterization, and Optical Properties of Monodisperse Chiral Oligofluorenes

Yanhou Geng,† Anita Trajkovska,† Dimitris Katsis,† Jane J. Ou,†
Sean W. Culligan,† and Shaw H. Chen*,†,‡

Contribution from the Department of Chemical Engineering and Laboratory for Laser Energetics, Center for Optoelectronics and Imaging, University of Rochester, 240 East River Road, Rochester, New York 14623-1212

Received March 11, 2002

Abstract: The first series of monodisperse chiral oligofluorenes was synthesized and characterized. Chain length was found to play an important role in solid morphology. Whereas dimer through tetramer are amorphous, pentamer through hexadecamer all show cholesteric mesomorphism with varying degrees of morphological stability against crystallization. Pristine spin-cast films, approximately 90 nm in thickness, are amorphous but exhibit pronounced circular dichroism and highly efficient circularly polarized fluorescence, suggesting the presence of chiral assemblies that remain to be experimentally characterized. A nonamer with two sets of the 2*S*-methylbutyl group replaced by the 3*S*,7-dimethyloctyl group was prepared and shown to be capable of forming a monodomain, glassy cholesteric film with thermal treatment. The cholesteric film is responsible for an order-of-magnitude increase in circular dichroism and a handedness reversal in circularly polarized fluorescence as compared to the amorphous pristine film. Molecular dynamics simulation furnished new insight into the molecular origin of the observed chiral optical properties in neat films.

I. Introduction

Because of the diverse structures and properties available through macromolecular design and synthesis, π-conjugated polymers have been intensively explored for electronics, optics, photonics, and optoelectronics over the past two decades.[1] Feasibility has been demonstrated for light-emitting diodes,[2] organic lasers,[3] thin film transistors,[4] photoconductors,[5] and nonlinear optical devices.[6] It has been shown that properties are affected by film morphology at a length scale from macroscopic down to a few angstroms, as determined by polymer structure and film processing conditions.[7,8] A particularly challenging aspect is the design of chiral conjugated systems directed at the formation of helices, twisted ribbons, and cholesteric mesomorphism in solution and neat film. Attempts have been made to interpret the supramolecular structures of poly(thiophene)s,[9−11] poly(*p*-phenylenevinylene)s,[12,13] poly(fluorene)s,[14] poly(*p*-phenylene)s,[15] and poly(acetylene)s,[16,17] all carrying enantiomeric pendants. Although both circular dichroism and circularly polarized fluorescence support some form of chiral structures,[10] few positive identifications have been achieved[15,17] presumably because of the difficulty encountered in aligning conjugated polymer films. To facilitate film processing for a systematic investigation of structure−property relationships and for practical applications, monodisperse chiral conjugated oligomers appear to be superior to conjugated polymers in general.[18] In particular, aggregate structures of helically shaped aromatic oligomers have been characterized by X-ray crystallography and electron microscopy.[19,20] Chiral sexithiophenes have also been reported to exhibit smectic mesomorphism but

* To whom correspondence should be addressed. E-mail: shch@lle.rochester.edu.
† Department of Chemical Engineering, University of Rochester.
‡ Laboratory for Laser Energetics, University of Rochester.

(1) *Semiconducting Polymers: Chemistry, Physics, and Engineering*; Hadzioannou, G., van Hutten, P. F., Eds.; Wiley-VCH: Weinheim, 2000.
(2) Friend, R. H.; Gymer, R. W.; Holmes, A. B.; Burroughes, J. H.; Marks, R. N.; Taliani, C.; Bradley, D. D. C.; Dos Santos, D. A.; Brédas, J. L.; Lögdlund, M.; Salaneck, W. R. *Nature* **1999**, *397*, 121.
(3) Tessler, N.; Denton, G. J.; Friend, R. H. *Nature* **1996**, *382*, 695.
(4) Horowitz, G. *Adv. Mater*. **1998**, *10*, 365.
(5) Strohriegl, P.; Grazulevicius, J. V. In *Handbook of Organic Conductive Molecules and Polymers*; Nalwa, H. S., Ed.; Wiley: Chichester, New York, 1997; Vol. 1, Chapter 11.
(6) Marder, S. R.; Kippelen, B.; Jen, A. K. Y.; Peyghambarian, N. *Nature* **1997**, *388*, 845.
(7) (a) Nguyen, T. Q.; Martini, I. B.; Liu, J.; Schwartz, J. *J. Phys. Chem. B* **2000**, *104*, 237. (b) Teetsov, J.; Vanden Bout, D. A. *J. Phys. Chem. B* **2000**, *104*, 9378.
(8) Kim, J.; Swager, T. M. *Nature* **2001**, *411*, 1030.
(9) Bouman, M. M.; Meijer, E. W. *Adv. Mater*. **1995**, *7*, 385.
(10) Langeveld, B. M. W.; Janssen, R. A. J.; Meijer, E. W. *J. Mol. Struct.* **2000**, *521*, 285.
(11) Zhang, Z. B.; Fujiki, M.; Motonaga, M.; Nakashima, H.; Torimitsu, K.; Tang, H. Z. *Macromolecules* **2002**, *35*, 941.
(12) Peeters, E.; Christiaans, M. P. T.; Janssen, R. A. J.; Schoo, H. F. M.; Dekkers, H. P. J. M.; Meijer, E. W. *J. Am. Chem. Soc*. **1997**, *119*, 9909.
(13) Meskers, S. C. J.; Peeters, E.; Langeveld, B. M. W.; Janssen, R. A. J. *Adv. Mater*. **2000**, *12*, 589.
(14) Oda, M.; Nothofer, H. G.; Lieser, G.; Scherf, U.; Meskers, S. C. J.; Neher, D. *Adv. Mater*. **2000**, *12*, 362.
(15) Chen, H. P.; Katsis, D.; Mastrangelo, J. C.; Marshall, K. L.; Chen, S. H.; Mourey, T. H. *Chem. Mater*. **2000**, *12*, 2275.
(16) Nakako, H.; Nomura, R.; Masuda, T. *Macromolecules* **2001**, *34*, 1496.
(17) Shinohara, K.; Yasuda, S.; Kato, G.; Fujita, M.; Shigekawa, H. *J. Am. Chem. Soc*. **2001**, *123*, 3619.
(18) Müllen, K.; Wegner, G. *Electronic Materials: The Oligomer Approach*; Wiley-VCH: Weinheim, New York, 1998.
(19) Lovinger, A. J.; Nuckolls, C.; Katz, T. J. *J. Am. Chem. Soc*. **1998**, *120*, 264.

Chart 1. Structure of Chiral Oligofluorenes and Polymer[a]

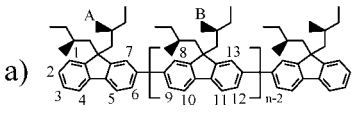

F(5*S*)–n
n=2–12, 16

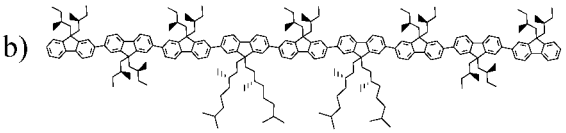

F(5*S*)7F(10*S*)2

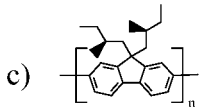

F(5*S*)-polymer

[a] (a) **F(5*S*)-n**, where A and B identify two types of methyl group, and 1−13 identify protons; (b) **F(5*S*)7F(10*S*)2**; (c) **(F(5*S*)-polymer**.

with a tendency to crystallize on cooling.[21] Chiroptical properties of other types of monodisperse conjugated oligomers in solution have also been characterized.[22,23] Of all the conjugated systems that have been explored, poly(fluorene)s have been identified as the prime candidate for electroluminescence, not only because of superior stability and efficiency to other conjugated polymers,[24−26] but also because of the potential for liquid-crystal-mediated alignment.[27,28] Amorphous oligofluorenes have also been synthesized to further improve on temporal stability of blue emission from neat films.[29,30] The objectives of this study are the following: to synthesize the first series of monodisperse chiral oligofluorenes, to investigate the effect of chain length on thermotropic and optical properties in dilute solution and neat film, to assess chiroptical properties in relation to the morphology of glassy films, and to furnish new insight into experimental observations through molecular simulation.

II. Results and Discussion

The general structure of oligofluorenes is depicted in Chart 1a as **F(5*S*)-n**, where n represents the number of fluorene units, and 5*S* represents the 2*S*-methylbutyl group. These compounds were synthesized following the divergent/convergent approach[31,32] as outlined in reaction Scheme 1. The dimer, **F(5*S*)-2**, was prepared from **1** in two steps. Comprising a trimethylsilyl protecting group, **4** was prepared by treating **3** with 1 equiv of *n*-BuLi followed by quenching with trimethylsilyl chloride. The boronic acid, **5**, prepared from **4** was coupled to **3** to obtain **6** and **7** upon separation and purification. Treatment of **6** and **7** with ICl afforded intermediates **9** and **10**, the two iodides intended to enhance selectivity and yield in the subsequent Suzuki coupling reaction.[33] Intermediate **12** was obtained in three steps from **6** and **9**. The trimer, **F(5*S*)-3**, along with **13**, was prepared through the Suzuki coupling reaction, and **13** was further converted to **14**. Similar procedures were followed for the preparation of **F(5*S*)-5**, **F(5*S*)-6**, **15**, **16**, and **19**−**22**. Treatment of **17** with BBr_3 afforded **F(5*S*)-4** and **18**. Oligofluorenes with an odd number of units, **F(5*S*)-7**, **F(5*S*)-9**, and **F(5*S*)-11**, were prepared by the Suzuki coupling reaction in a 39−48% yield, whereas those with an even number, **F(5*S*)-8**, **F(5*S*)-12**, and **F(5*S*)-16**, were prepared by the Yamamoto coupling reaction[34] in a 43−83% yield. In general, the higher oligomers required an increasing equivalent of catalyst to arrive at a comparable yield with the lower oligomers. Molecular structures were elucidated with elemental analysis and ^{1}H NMR spectroscopy.

Analysis based on both high performance liquid chromatography and size exclusion chromatography indicated an absence of precursors and a purity level of better than 99%. Parts of the ^{1}H NMR spectra of **F(5*S*)-2**, **-4**, **-8**, and **-16** were displayed in Figure 1 for a quantitative assessment of peak integrations in comparison to the chemical formulas. The peaks between δ 7.28 and 7.45 and those between δ 0.25 and 0.45 are attributed, respectively, to the protons in terminal fluorene units, identified as 1−3, and the 2-methyl groups, identified as A and B in Chart 1a.[35,36]

Good agreement between the calculation and observation of peak integrations is shown in Table 1. In view of the general tendency of **F(5*S*)-n** to crystallize upon heating, **F(5*S*)7F(10*S*)-2**, as depicted in Chart 1b, was synthesized following reaction Scheme 2, to enable the preparation of a glassy, monodomain cholesteric film via spin coating and subsequent thermal annealing.

Phase transition temperatures were determined with differential scanning calorimetry in conjugation with hot-stage polarizing optical microscopy, and the results are summarized in Table 2. All of the samples were preheated to 370 °C with subsequent cooling to −30 °C at a rate of −20 °C/min before gathering the second heating scan at 20 °C/min. With cholesteric mesomorphism identified as oily streaks, the second heating and the first cooling scans are reported as the first and second line, respectively, for each sample in Table 2.

Lower oligomers are amorphous with a glass transition temperature, T_g, increasing in the order **F(5*S*)-2** < **F(5*S*)-3** < **F(5*S*)-4** without crystallization or liquid crystalline mesomor-

(20) (a) Berl, V.; Huc, I.; Khoury, R. G.; Lehn, J. M. *Chem.-Eur. J.* **2001**, *7*, 2798. (b) Ohkita, M.; Lehn, J. M.; Baum, G.; Fenske, D. *Chem.-Eur. J.* **1999**, *5*, 3471.
(21) Schenning, A. P. H. J.; Kilbinger, A. F. M.; Biscarini, F.; Cavallini, M.; Cooper, H. J.; Derrick, P. J.; Feast, W. J.; Lazzaroni, R.; Leclère, Ph.; McDonell, L. A.; Meijer, E. W.; Meskers, S. C. J. *J. Am. Chem. Soc*. **2002**, *124*, 1269.
(22) (a) Prince, R. B.; Brunsveld, L.; Meijer, E. W.; Moore, J. S. *Angew. Chem., Int. Ed.* **2000**, *39*, 228. (b) Brunsveld, L.; Meijer, E. W.; Prince, R. B.; Moore, J. S. *J. Am. Chem. Soc*. **2001**, *123*, 7978.
(23) Sakurai, S.; Goto, H.; Yashima, E. *Org. Lett.* **2001**, *3*, 2379.
(24) Klärner, G.; Lee, J.-K.; Davey, M. H.; Miller, R. D. *Adv. Mater*. **1999**, *11*, 115.
(25) Yu, W. L.; Pei, J.; Huang, W.; Heeger, A. J. *Adv. Mater*. **2000**, *12*, 828.
(26) Virgili, T.; Lidzey, D. G.; Bradley, D. D. C. *Adv. Mater*. **2000**, *12*, 58.
(27) Whitehead, K. S.; Grell, M.; Bradley, D. D. C.; Jandke, M.; Strohriegl, P. *Appl. Phys. Lett*. **2000**, *76*, 2946.
(28) Grell, M.; Knoll, W.; Lupo, D.; Meisel, A.; Miteva, T.; Neher, D.; Nothofer, H. G.; Scherf, U.; Yasuda, A. *Adv. Mater*. **1999**, *11*, 671.
(29) Weinfurtner, K. H.; Weissörtel, F.; Harmgarth, G.; Salbeck, J. *Proc. SPIE* **1998**, *3476*, 40.
(30) (a) Geng, Y. H.; Katsis, D.; Culligan, S. W.; Ou, J. J.; Chen, S. H.; Rothberg, L. J. *Chem. Mater*. **2002**, *14*, 463. (b) Katsis, D.; Geng, Y. H.; Culligan, S. W.; Trajkovska, A.; Chen, S. H.; Rothberg, L. J. *Chem. Mater*. **2002**, *14*, 1332.
(31) (a) Pearson, D. L.; Tour, J. M. *J. Org. Chem*. **1997**, *62*, 1376. (b) Jones, L.; Schumn, J. S.; Tour, J. M. *J. Org. Chem*. **1997**, *62*, 1388.
(32) (a) Hensel, V.; Schluter, A. D. *Chem.-Eur. J*. **1999**, *5*, 421. (b) Liess, P.; Hensel, V.; Schluter, A. D. *Liebigs Ann*. **1996**, 1037.
(33) Miyaura, N.; Suzuki, A. *Chem. Rev*. **1995**, *95*, 2457.
(34) Yamamoto, T.; Morita, A.; Miyazaki, Y.; Maruyama, T.; Wakayama, H.; Zhou, Z.-H.; Nakamura, Y.; Kanbara, T.; Sasaki, S.; Kubota, K. *Macromolecules* **1992**, *25*, 1214.
(35) Fukuda, M.; Sawada, K.; Yoshino, K. *J. Polym. Sci., Part A: Polym. Chem*. **1993**, *31*, 2465.
(36) Ranger, M.; Leclerc, M. *Macromolecules* **1999**, *32*, 3306.

Scheme 1. Synthesis of Oligofluorenes, **F(5*S*)-*n***[a]

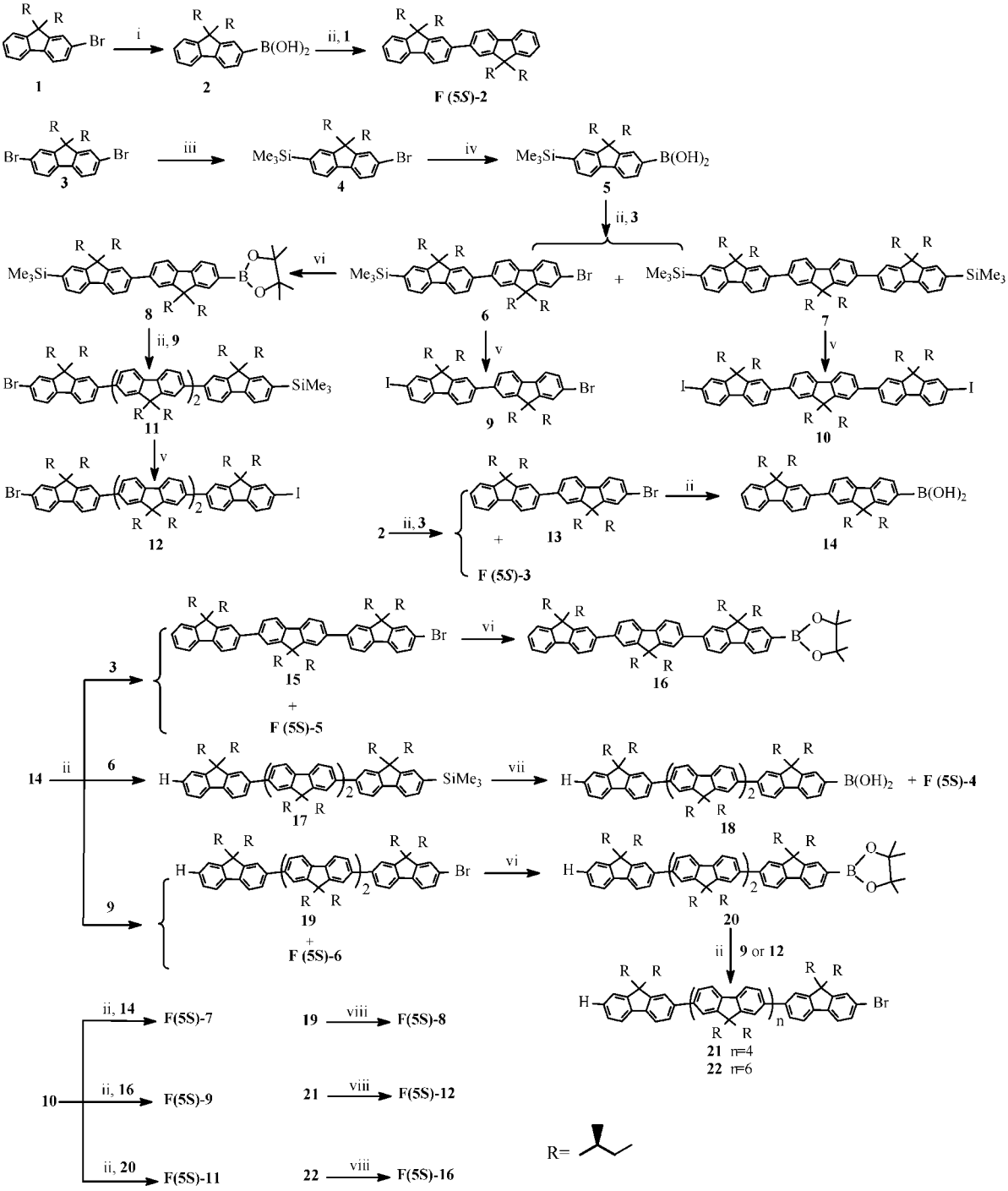

[a] (i) (1) *n*-BuLi, −78 °C; (2) (*i*-PrO)$_3$B, −78 °C to room temperature; (3) H_3O^+. (ii) $Pd(PPh_3)_4$, Na_2CO_3 (2.0 M aqueous), 90 °C. (iii) (1) *n*-BuLi, −78 °C; (2) $ClSiMe_3$, −78 °C to room temperature. (iv) (1) *n*-BuLi, −78 °C; (2) (*i*-PrO)$_3$B, −78 °C to room temperature; (3) H_2O. (v) ICl, 0 °C. (vi) (1) *n*-BuLi, −78 °C; (2) 2-isopropoxy-4,4,5,5-tetramethyl-1,3,2-dioxaborolane, −78 °C to room temperature. (vii) (1) BBr_3, room temperature; (2) H_2O. (viii) Ni(COD)/2,2′-bipyridine/COD, 80 °C.

phism. All of the oligomers longer than four fluorene units are inherently mesomorphic. Whereas **F(5*S*)-5** is the only sample that resists crystallization on heating, cholesteric fluids of **F-(5*S*)-5**, **-6**, **-7**, and **-8** showed an increasing T_g on cooling without encountering crystallization.

To illustrate the ability of these oligomers to preserve cholesteric structure in the solid state, a micron thick film of **F(5*S*)-8** was contained between a microscope slide and a cover slip without alignment coating to encourage formation of disclinations. The sandwiched films were annealed at 300 °C for $^1/_2$ h before quenching to room temperature. The presence of oily streaks along with the absence of crystallinity observed under polarizing optical microscopy confirms that crystallization could be avoided in the quenching process. To measure the helical pitch length, p, a 4 μm thick film contained between surface-treated silica substrates was prepared following the same melt processing. The resultant well-aligned film was monodomain (i.e., devoid of oily streaks). The SEM image of the film's cross section revealed that $p = 123 \pm 7$ nm, a value also observed for a **F(5*S*)-5** film. In contrast, **F(5*S*)-9**, **-11**, **-12**, and

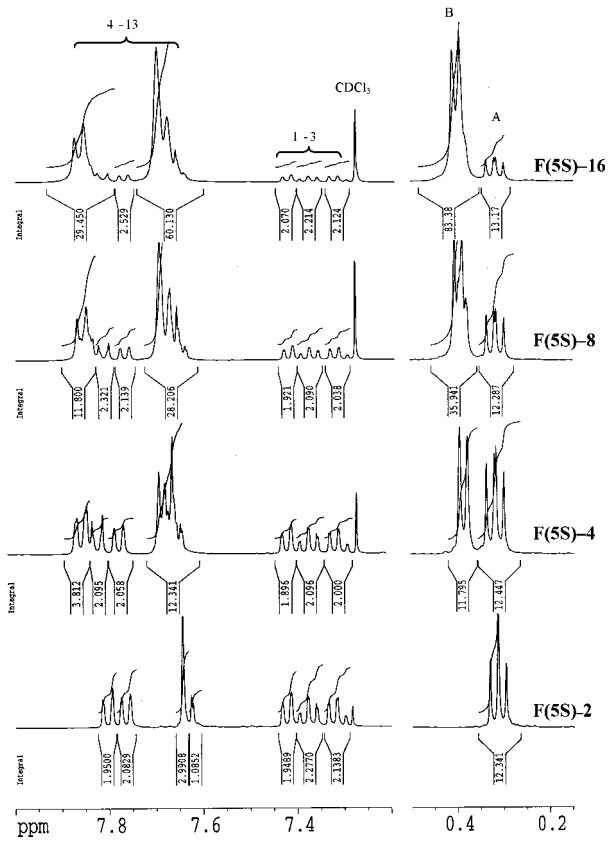

Figure 1. ^{1}H NMR spectra ($CDCl_3$, 400 MHz) of **F(5*S*)-n**, n = 2, 4, 8, and 16, with chain lengths verified by integrations of signals identified as A, B, 1−3, and 4−13.

Table 1. End-Group Analysis of ^{1}H NMR Spectra To Validate the Chain Lengths of Oligo[(2*S*-methylbutyl)fluorene]s

sample		CH_3(A)	CH_3(B)	H(1–3)	H(4–13)
F(5*S*)-2	calc	12	0	6	8
	obsd	12.3	0	6.3	8.0
F(5*S*)-4	calc	12	12	6	20
	obsd	12.4	11.8	6.0	20.2
F(5*S*)-8	calc	12	36	6	44
	obsd	12.3	35.9	6.0	44.4
F(5*S*)-16	calc	12	84	6	92
	obsd	13.2	83.4	6.4	92.0

-16 and a polymer analogue (depicted in Chart 1c with $\bar{M}_w$ = 35 100 and $\bar{M}_n$ = 21 500 g/mol, equivalent to **F(5*S*)-70**) all tend to crystallize both on heating and on cooling, thus preventing a glassy cholesteric film from being prepared by melt processing.

To furnish insight into the nature of chiral structures consisting of oligofluorenes, micron thick films are not appropriate for circular dichroism or circularly polarized fluorescence because of the excessive absorbance. Instead of melt processing, spin coating from 1 wt % chloroform solutions was carried out for the preparation of approximately 90 nm thick, neat films. Light absorption and fluorescence (with an excitation wavelength of 370 nm) spectra were gathered for the pristine films of all oligomers. Typical results are shown in Figure 2 for a pristine **F(5*S*)-16** film, which was characterized to be amorphous by polarizing optical microscopy and electron diffraction (see inset in Figure 2a). As shown in Table 2, the maximum wavelengths in absorption (λ_{max}^{abs}) and fluorescence (λ_{max}^{flu}) increase with chain length as expected. For a given sample, neat film and dilute solution (10^{-6} M fluorene units in chloroform) show nearly identical λ_{max}^{abs} values, indicating an absence of ground-state aggregation in the solid state. However, neat film shows a 5−9 nm red shift in λ_{max}^{flu} from dilute solution at the same chain length, suggesting light emission from a more planar structure in the solid state. The general trends exhibited by λ_{max}^{abs} and λ_{max}^{flu} in dilute solution with respect to chain length are consistent with a recent report on monodisperse oligo[9,9-bis(*n*-hexyl)fluorene]s.[37] As also shown in Table 2, the fluorescence quantum yields of chiral oligomers (0.51−0.85) are superior to that of their polymer analogue (0.24) with the average refractive indices measured by variable angle spectroscopic ellipsometry. One plausible explanation is that the polymer film contains aggregates, formed during the spin-coating process, that act as fluorescence quenching sites,[7] which are apparently absent in oligomer films. These amorphous, spin-cast films were further characterized in terms of circular dichroism (CD) and circularly polarized fluorescence (CPF) with the spectra illustrated in Figure 2b and c for a **F(5*S*)-16** film. The bisignate CD spectrum as shown in Figure 2b suggests the presence of chiral assemblies in neat film. In contrast, vanishing CD values were observed in chloroform (a good solvent) containing up to 30% methanol (a poor solvent). The same neat film of **F(5*S*)-16** gave rise to strong CPF as shown in Figure 2c. The pronounced CPF as well as bisignate CD must have originated from some form of supramolecular chirality.

Presented in Figure 3a are the CD spectra of **F(5*S*)-5**, **-7**, **-9**, **-12**, and **-16** of approximately the same film thickness (90 ± 4 nm) determined with ellipsometry. The negative peaks centering around 410 nm suggest a left-handed orientation between chromophores based on exciton coupling theory,[38a] but the structure of these chiral assemblies remains to be experimentally characterized. The fact that the CD spectra collectively define an "isodichroic point" suggests similar chiral assemblies with a longer chain supporting an increasing extent of handedness preference.[22] However, handedness preference appears to be saturated at **F(5*S*)-12** because of the inevitable defects, such as kinks and reversals.[38b] In contrast to oligomers, the amorphous polymer film exhibits a relatively weak CD signal while missing the isodichroic point, suggesting that polymer chains assume dissimilar chiral structures to oligomers. The degree of CPF can be quantified by the dissymmetry factor, $g_e \equiv 2(I_L - I_R)/(I_L + I_R)$, where I_L and I_R are left- and right-handed circularly polarized intensity, respectively. The CPF spectra, as illustrated in Figure 2c for **F(5*S*)-16**, were employed to calculate g_e, as compiled in Figure 3b for selected samples.

Note that the g_e value increases with oligomer's chain length, but that it vanishes in the polymer analogue. Because all of the chiral oligofluorenes except **F(5*S*)-2**, **-3**, and **-4** exhibit cholesteric mesomorphism at elevated temperatures (i.e., above T_g or above the crystalline melting point, T_m), attempts were made to prepare glassy cholesteric films via thermal annealing of spin-cast films followed by quenching. However, annealing above T_g did not result in monodomain cholesteric film without encountering thermally activated crystallization or destroying the film's integrity (at elevated temperatures).

(37) Klärner, G.; Miller, R. D. *Macromolecules* **1998**, *31*, 2007.
(38) (a) Berova, N.; Nakanishi, K. In *Circular Dichroism: Principles and Applications*, 2nd ed.; Berova, N., Nakanishi, K., Woody, R. W., Eds.; Wiley-VCH: New York, 2000; Chapter 12. (b) Green, M. M. In *Circular Dichroism: Principles and Applications*, 2nd ed.; Berova, N., Nakanishi, K., Woody, R. W., Eds.; Wiley-VCH: New York, 2000; Chapter 17.

Scheme 2. Synthesis of **F(5*S*)7F(10*S*)2**[a]

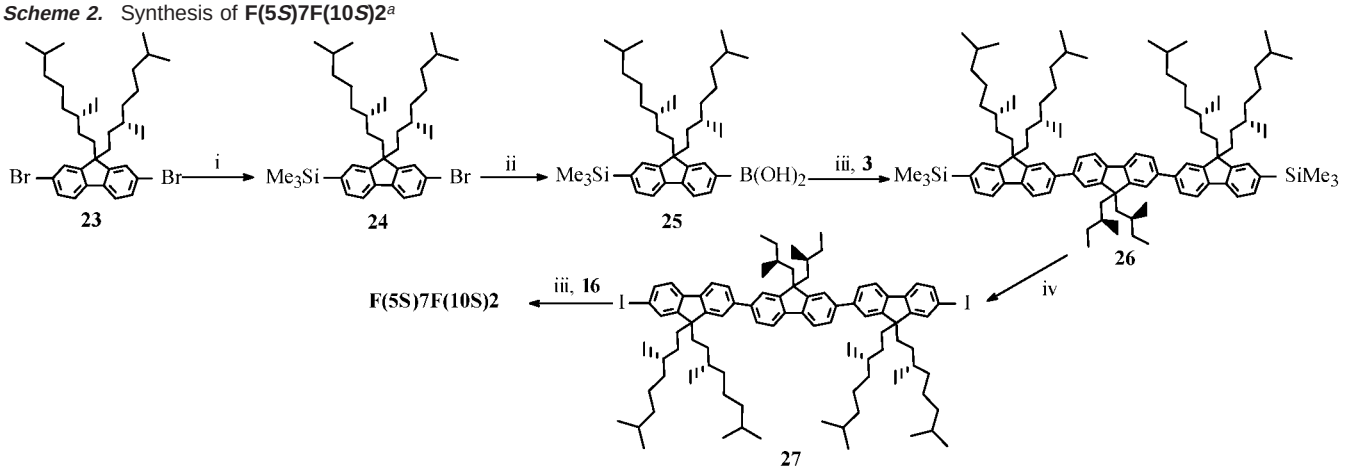

[a] (i) (1) *n*-BuLi, −78 °C; (2) $ClSiMe_3$, −78 °C to room temperature. (ii) (1) *n*-BuLi, −78 °C; (2) (*i*-PrO)$_3$B, −78 °C to room temperature; (3) H_2O. (iii) $Pd(PPh_3)_4$, Na_2CO_3 (2.0 M aqueous), 90 °C. (iv) ICl, 0 °C.

Table 2. Thermal Transition Temperatures, Light Absorption, and Fluorescence (Excitation at 370 nm) Properties in Chloroform (10^{-6} M in Fluorene Units) and Spin-Cast Films

		solution			film				
sample	phase transition temperatures	λ_{max}^{abs}, nm	λ_{max}^{flu}, nm		thickness, nm	λ_{max}^{abs}, nm	λ_{max}^{flu}, nm		quantum yield (film)
F(5*S*)-2	*G* 15 °C *I* *I* 8 °C *G*	330	363	383					
F(5*S*)-3	*G* 40 °C *I* *I* 29 °C *G*	350	390	413		349	398	418	
F(5*S*)-4	*G* 80 °C *I* *I* 70 °C *G*	361	403	427	91	360	409	432	0.75
F(5*S*)-5	*G* 95 °C *Ch* 176 °C *I*[a] *I* 170 °C *Ch* 87 °C *G*	366	408	432	87	366	415	439	0.76 ± 0.08
F(5*S*)-6	*G* 110 °C *Ch*, 200 °C *K* 221 °C *Ch* 265 °C *I*[b] *I* 261 °C *Ch* 101 °C *G*	370	410	433		369	415	440	
F(5*S*)-7	*G* 118 °C *Ch*, 153 °C K_1 222 °C K_2 231 °C *Ch* 331 °C *I* *I* 326 °C *Ch* 110 °C *G*	374	410	435	95	372	417	442	0.83
F(5*S*)-8	*G* 124 °C *Ch*, 144 °C *K* 236 °C *Ch* *Ch* 120 °C *G*	375	412	435	98	374	419	442	0.85
F(5*S*)-9	*K* 254 °C *Ch*[c] *Ch* 170 °C *K*	377	412	436	88	376	420	442	0.67 ± 0.03
F(5*S*)-11	*K* 271 °C *Ch* *Ch* 208 °C *K*	379	412	436	85	377	418	442	0.51 ± 0.01
F(5*S*)-12	*K* 273 °C *Ch* *Ch* 220 °C *K*	379	411	435	88	378	418	443	
F(5S)-16	*K* 294 °C *Ch* *Ch* 259 °C *K*	382	412	437	91	379	420	443	
F(5S)-polymer	*K* 349 °C *Ch* *Ch* 279 °C *K*	387	414	438	116	379	423	444	0.24

[a] The first line reports a heating scan at 20 °C/min of a sample preheated to 370 °C followed by cooling at −20 °C/min to −30 °C, which is reported in the second line. Symbols: *G*, glassy; *Ch*, cholesteric; *I*, isotropic; *K*, crystalline. [b] The second heating scan at 20 °C/min showed glass transition to a cholesteric fluid at 110 °C followed by crystallization at 200 °C, melting into a cholesteric fluid at 221 °C, and clearing at 265 °C; the cooling scan at −20 °C/min showed an isotropic-to-cholesteric transition at 261 °C followed by glass transition at 101 °C. [c] The first line reports the second heating scan at 20 °C/min, showing crystalline melting at 254 °C into a cholesteric fluid which persists till thermal decomposition at 375 °C; the second line reports a cooling scan at −20 °C/min showing a cholesteric-to-crystalline transition at 170 °C.

To suppress the oligomers' propensity to crystallize, some of the 2*S*-methylbutyl groups were replaced with 3*S*,7-dimethyloctyl groups, such as **F(5*S*)7F(10*S*)2** depicted in Chart 1b and synthesized according to reaction Scheme 2. The DSC second heating scans compiled in Figure 4 indicate that the cholesteric fluid of **F(5*S*)7F(10*S*)2** resists crystallization on heating and cooling, in contrast to **F(5*S*)-n** with n ≥ 9 that tend to crystallize on heating and cooling.

The absence of crystallization characteristic of **F(5*S*)7F(10*S*)-2** facilitates the identification of cholesteric mesomorphism with oily streaks (Figure 5a) and processing into monodomain films (Figure 5b), which in turn provides an SEM image (Figure 5c) of the film cross section yielding $p = 180$ nm.

This helical pitch length is longer than that of **F(5*S*)-8**, consistent with the fact that poly(fluorene) with pendant 3*S*,7-dimethyloctyl groups shows opposite signs in chiroptical properties to those with pendant 2*S*-methylbutyl groups.[14] Unlike the pristine, spin-cast films of **F(5*S*)-n** and their polymer analogue, **F(5*S*)7F(10*S*)2**, resulted in a weakly anisotropic, spin-cast film under polarizing optical microscopy, suggesting a complex morphology that renders spectroscopic ellipsometry inapplicable. Thermal annealing of the pristine film at 95 °C

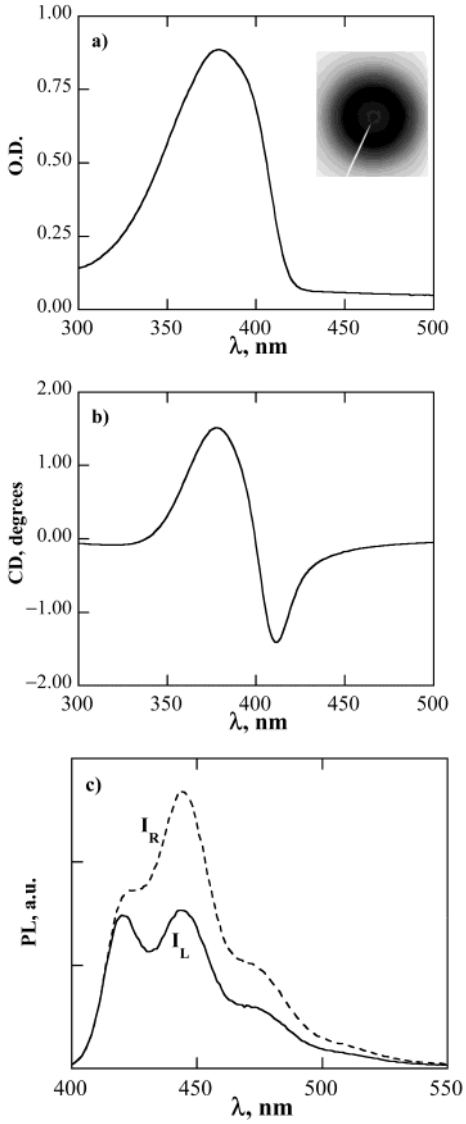

Figure 2. Optical properties of a pristine, spin-cast 91 nm thick film of **F(5*S*)-16**: (a) UV−vis absorption spectrum with electron diffraction pattern (as inset) showing film's amorphous character; (b) circular dichroism spectrum; and (c) circularly polarized fluorescence spectrum (with unpolarized excitation at 370 nm).

for $^1/_2$ h produced an optically anisotropic film, for which the ellipsometric data were collected. In light of Figure 5 collected for a 4 μm thick sandwiched film, the annealed spin-cast film was modeled as a cholesteric stack. To treat the ellipsometric data of a cholesteric film, the dispersion of both the ordinary (n_o) and the extraordinary (n_e) refractive indices of the quasinematic layer within a cholesteric stack was measured for a monodomain, glassy nematic film prepared with **F(5)7F(8)2** as depicted in Figure 6a; note the structural similarity between **F(5)7F(8)2** and **F(5*S*)7F(10*S*)2**. Because the synthesis and properties of a series of related materials will be published elsewhere, it suffices to mention here that **F(5)7F(8)2** has its molecular structure validated with elemental analysis and ^{1}H NMR spectroscopy[39] and that it undergoes glass transition at

(39) Culligan, S. W.; Geng, Y. H.; Katsis, D.; Chen, S. H., manuscript in preparation. The molecular structure of **F(5)7F(8)2** is elucidated as follows. ^{1}H NMR (400 MHz, $CDCl_3$): δ (ppm) 7.83−7.87 (m, 14H), 7.82 (d, J = 8.28 Hz, 2H), 7.77 (d, J = 7.41 Hz, 2H), 7.61−7.73 (m, 32H), 7.29−7.48 (m, 6H), 1.88−2.38 (m, 36H), 0.58−1.18 (m, 144H), 0.26−0.46 (m, 42H). Anal. Calcd for $C_{219}H_{278}$: C, 90.37; H, 9.63. Found: C, 90.37; H, 9.49.

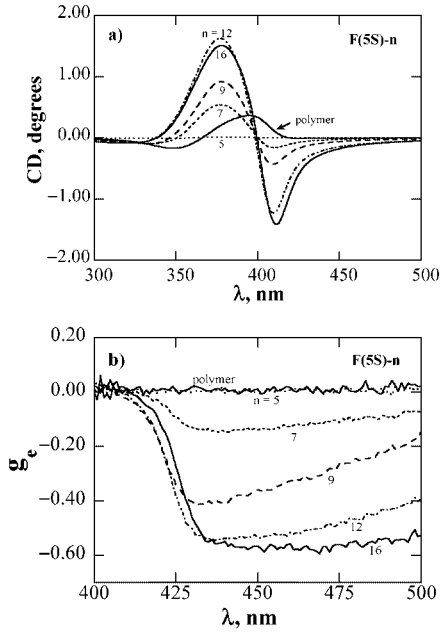

Figure 3. Chiroptical properties of pristine films of **F(5*S*)-n**, n = 5, 7, 9, 12, and 16 (90 ± 4 nm in thickness), and that of a polymer analogue (116 nm in thickness) with a number-average chain length of 70: (a) circular dichroism spectra; and (b) dissymmetry factor, g_e, with unpolarized excitation at 370 nm.

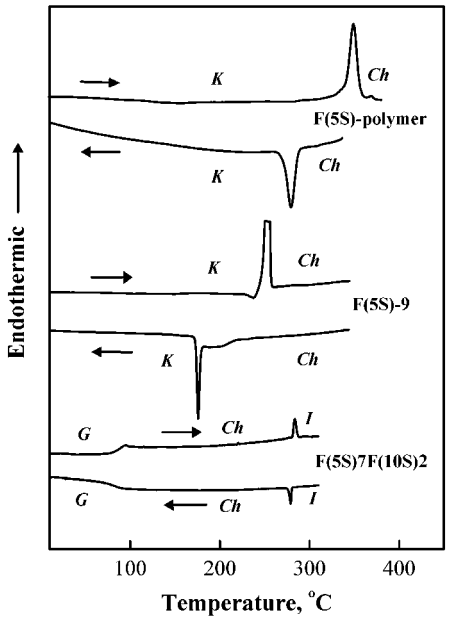

Figure 4. The DSC heating scans at 20 °C/min of samples of **F(5*S*)7F-(10*S*)2**, **F(5*S*)-9**, and its polymer analogue, **F(5*S*)-polymer**, preheated to 370 °C followed by cooling at −20 °C/min to −30 °C, as also included. Symbols: *G*, glassy; *Ch*, cholesteric; *I*, isotropic; *K*, crystalline.

110 °C with nematic mesomorphism persisting beyond 350 °C. The absorption coefficients parallel ($\alpha_{||}$) and perpendicular ($\alpha_\perp$) to the nematic director, shown in Figure 6c as fitted parameters to the ellipsometric data, yielded an orientational order parameter $S = 0.83 \pm 0.01$ in a 92 nm thick spin-cast film annealed at 115 °C for $^1/_2$ h, a manifestation of the ease of aligning conjugated oligomers. The resultant S value agrees with S = 0.82 independently evaluated by UV−vis linear dichroism.

The absorption and CD spectra of the pristine and annealed films of **F(5*S*)7F(10*S*)2** are presented in Figure 7. Similar to a uniaxially ordered film of poly[9,9-bis(*n*-octyl)fluorene],[40] hy-

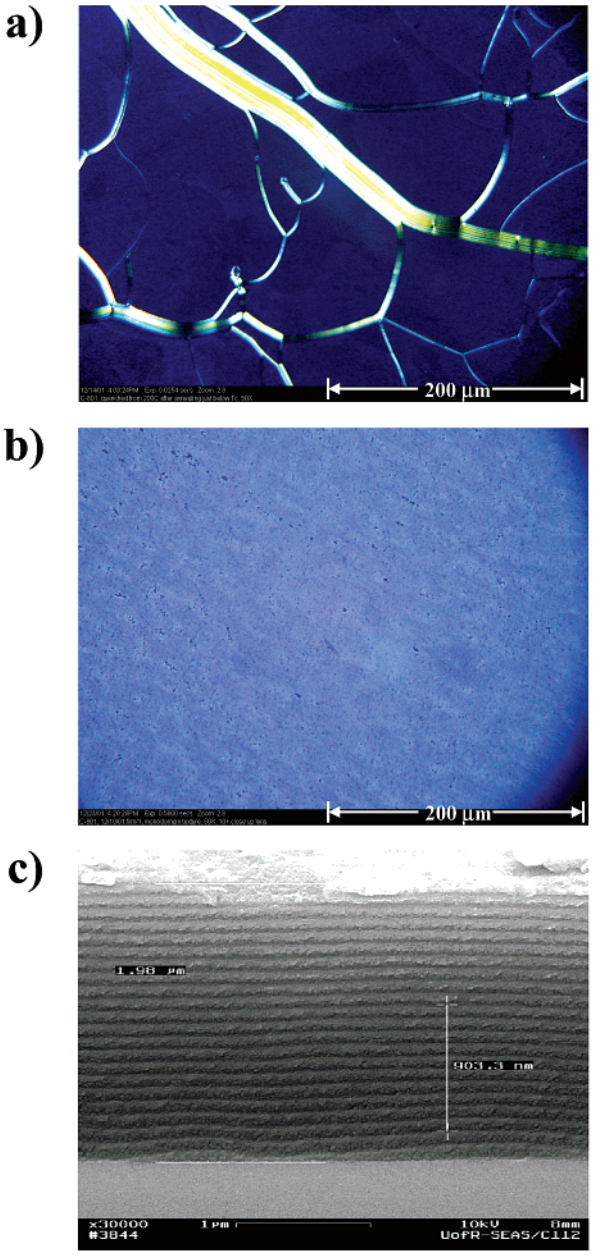

Figure 5. Micrographs of films of **F(5*S*)7F(10*S*)2**: (a) oily streaks characteristic of cholesteric mesomorphism observed under polarizing optical microscopy of a micron thick film contained between untreated glass slide and a cover slip; (b) a 4 μm thick film contained between surface-treated fused silica substrates, annealed at 200 °C for $^1/_2$ h followed by cooling at −6 °C/min to room temperature, resulting in a monodomain glassy cholesteric film observed under polarizing optical microscopy; (c) the SEM image of the cross section of the well-aligned film as described in (b).

pochromism was observed (see Figure 7a) as a result of thermal annealing. Thermal annealing also resulted in an order-of-magnitude increase in circular dichroism (from 0.9 to 12.8°) accompanied by a disappearance of the signature of exciton coupling at 415 nm exhibited by the pristine film.

With the dispersion curves of n_o and n_e shown in Figure 6b, the ellipsometric data gathered for an annealed, spin-cast film of **F(5*S*)7F(10*S*)2** were successfully modeled, yielding a thickness of 87 nm and a right-handed cholesteric structure with a pitch length of 333 nm. The Good−Karali theory[41] was then

(40) Teetsov, J.; Fox, M. A. *J. Mater. Chem.* **1999**, *9*, 2117.
(41) Good, R. H., Jr.; Karali, A. *J. Opt. Soc. Am. A* **1994**, *11*, 2145.

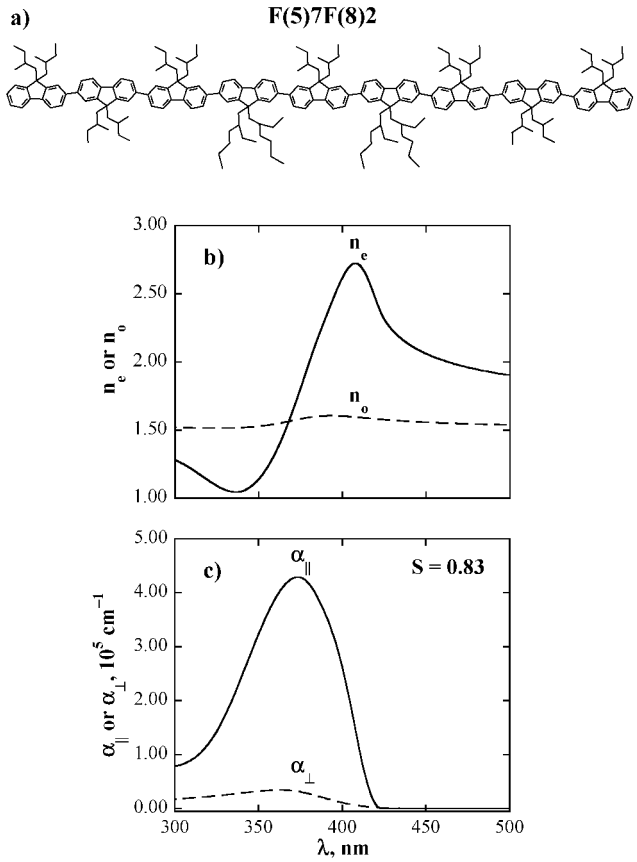

Figure 6. Ellipsometric characterization of a 92 nm thick nematic film of **F(5)7F(8)2** annealed at 115 °C for $^1/_2$ h: (a) its molecular structure; (b) extraordinary (n_e) and ordinary (n_o) refractive indices; and (c) absorption coefficients parallel ($\alpha_{||}$) and perpendicular ($\alpha_{\perp}$) to the nematic director.

used to predict the annealed film's CD spectrum with refractive indices, absorption coefficients, helical sense, pitch length, and film thickness as the input data.[42] The good agreement between theory and experiment shown in Figure 7b (dotted vs dashed curve) validates the treatment of the annealed film as a cholesteric stack. A comparison of the pristine film's CD spectrum (see the solid curve in Figure 7b) with those of the pristine films of **F(5*S*)-n** displayed in Figure 3a seems to indicate a composite morphology of a cholesteric stack and chiral assemblies with a left-handed orientation between chromophores as referred to earlier.

The implications of cholesteric structure are revealed in Figure 8. With photoexcitation at 370 nm, the g_e value undergoes a crossover from −0.15 to +0.75 accompanied by a slight decrease in fluorescence quantum yield from 0.82 to 0.67 caused by annealing. It is also noted that the pristine films of **F(5*S*)-n** with n ≥ 9 and both the pristine and the thermally annealed film of **F(5*S*)7F(10*S*)2** showed superior stability of blue emission when left under ambient condition over a period of months.

To address the questions of why amorphous films of oligofluorenes exhibit pronounced chiroptical properties and why an amorphous film of **F(5*S*)7F(10*S*)2** can be thermally processed into a monodomain cholesteric stack but not those of **F(5*S*)-*n***, molecular simulation was performed using the AMBER software package. Molecular mechanics computation revealed

(42) Conger, B. M. Ph.D. Thesis, University of Rochester, 1998.

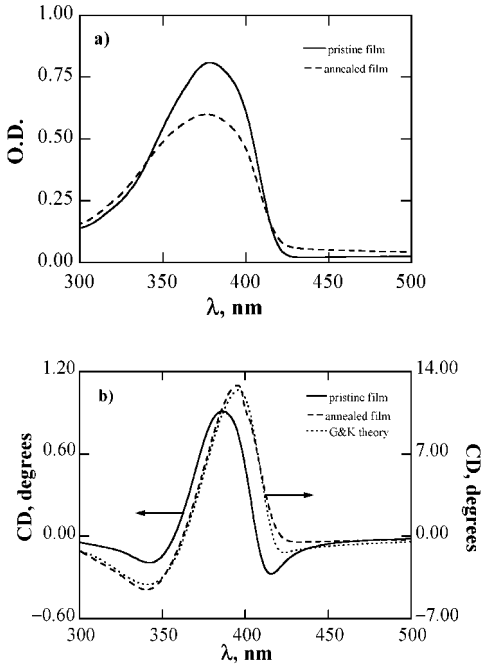

Figure 7. The effects of thermal annealing at 95 °C for $^1/_2$ h on optical properties of an 87 nm thick spin-cast film of **F(5*S*)7F(10*S*)2**: (a) UV−vis absorption spectra; and (b) circular dichroism spectra including a prediction based on the Good−Karali theory.

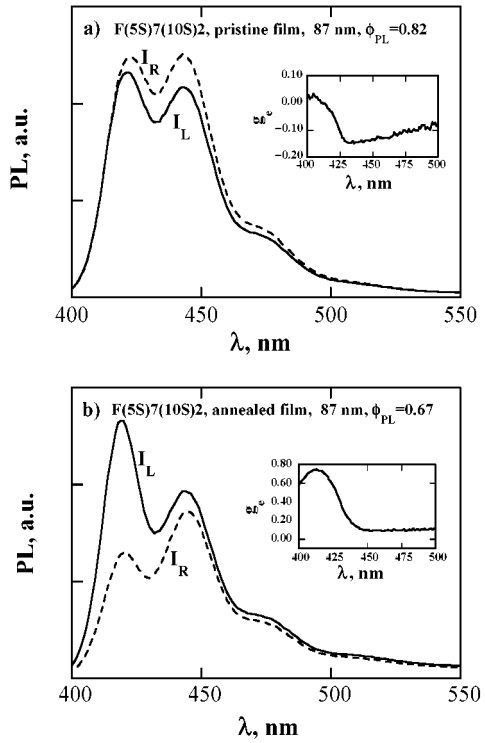

Figure 8. Circularly polarized fluorescence spectra of the same **F(5*S*)7F(10*S*)2** film reported in Figure 7: (a) pristine film; and (b) thermally annealed film. The dissymmetry factors are included as insets.

left-handed helices adopted by single molecules of **F(5*S*)-9** and **F(5*S*)7F(10*S*)2**. In both material systems, four energy-minimized molecules were included in the subsequent molecular dynamics computation. It is evident that molecules of **F(5*S*)-9** form braided chiral assemblies (see Figure 9a), while each molecule assumes a left-handed helical conformation, leading to the negative g_e profile shown in Figure 3b. However,

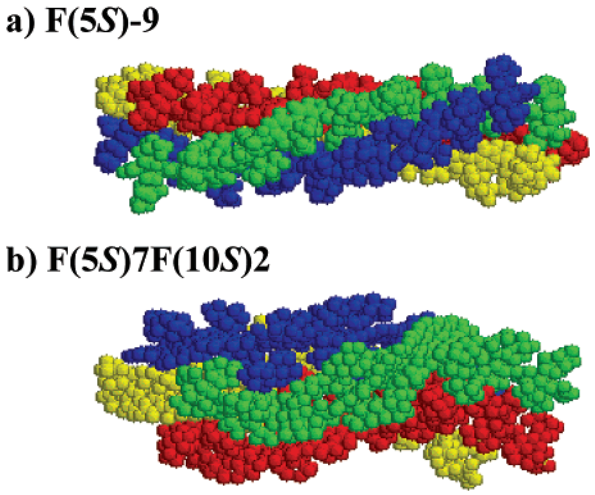

Figure 9. Molecular dynamics simulation of four molecules of monodisperse oligofluorenes using the AMBER software package: (a) **F(5*S*)-9**; and (b) **F(5*S*)7F(10*S*)2**.

molecules of **F(5*S*)7F(10*S*)2** are not braided (see Figure 9b), but each retains a left-handed helix, yielding the negative g_e profile shown in Figure 8a. Apparently, the difference in the molecular packing behavior between the two oligofluorenes arises from the relatively bulky 3*S*,7-dimethyloctyl group.

Molecular organization induced by thermal annealing of the loosely pitched, left-handed helices comprising unconstrained molecules in **F(5*S*)7F(10*S*)2** results in a right-handed cholesteric stack, which is responsible for the positive g_e profile shown in Figure 8b. The observed handedness reversal accompanying the transition from helical coils to a cholesteric stack is dictated by the energetics of molecular packing.[43] In the case of **F(5*S*)-9**, molecules are constrained in braided assemblies and do not have sufficient thermal energy to reorganize during annealing, thus failing to form a cholesteric stack.

III. Conclusions

The first series of monodisperse chiral oligofluorenes was synthesized following the divergent/convergent approach to investigate the role played by chain length in morphology and optical properties. Thermotropic properties were characterized by hot-stage polarizing optical microscopy and differential scanning calorimetry. Moreover, scanning electron microscopy was employed for the determination of helical pitch length in well-aligned cholesteric films. Spin-cast films were characterized in terms of circular dichroism, circularly polarized fluorescence, electron diffraction, and variable angle spectroscopic ellipsometry. Fundamental insight into chiroptical properties was also furnished through molecular dynamics simulation of multimolecular systems. Key observations are recapitulated as follows:

(1) Whereas dimer through tetramer are amorphous, all higher oligomers form cholesteric mesomorphism with varying degrees of morphological stability against crystallization. Pentamer resists crystallization on both heating and cooling, hexamer through octamer undergo crystallization on heating but not cooling, and nonamer through hexadecamer and polymer all tend to crystallize on both heating and cooling. In all cases, phase transition temperatures increase with chain length.

(43) Sato, T.; Sato, Y.; Umemura, Y.; Teramoto, A.; Nagamura, Y.; Wagner, J.; Weng, D.; Okamoto, Y.; Hatada, K.; Green, M. M. *Macromolecules* **1993**, *26*, 4551.

(2) Pristine, spin-cast films are amorphous with no spectral shift in UV−vis absorption but a 5−9 nm red shift in fluorescence as compared to the dilute solution data. The observed significant degrees of circular dichroism and circularly polarized fluorescence in approximately 90 nm thick films suggest the presence of chiral assemblies in the solid state. However, a vanishing degree of circularly polarized fluorescence was observed with a pristine polymer film. None of the oligo[9,9-bis(2*S*-methylbutyl)fluorene]s can be processed into ordered films via thermal annealing above T_g without encountering crystallization. In the absence of "aggregates" as quenching sites, the pristine oligomer films are more efficient light-emitters than the polymer analogue, $\Phi_{PL} = 0.51-0.85$ in comparison to 0.24.

(3) A nonamer with two sets of the 2*S*-methylbutyl group replaced by the 3*S*,7-dimethyloctyl group shows cholesteric mesomorphism without crystallization on heating and cooling. Moreover, thermal annealing of a spin-cast film yields an ordered film. Ellipsometric analysis and modeling of the circular dichroism data based on the Good−Karali theory suggest a right-handed cholesteric structure for the annealed film. The emerging cholesteric structure is responsible for an order-of-magnitude increase in circular dichroism (from 0.9 to 12.8°) and a handedness reversal in circularly polarized fluorescence (g_e from −0.15 to +0.75). The thermally annealed film's circularly polarized fluorescence spectra are consistent with a right-handed cholesteric structure, while the nature of chiral assemblies in the pristine film, as those of oligo[9,9-bis(2*S*-methylbutyl)-fluorene]s, remains to be experimentally characterized.

(4) Molecular dynamics simulation reveals the structures of chiral assemblies that have escaped experimental characterization thus far. Molecules in the pristine, spin-cast film of the nonamer carrying 2*S*-methylbutyl pendants form braided chiral assemblies, while each molecule assumes a left-handed helix. Insertion of the bulky 3*S*,7-dimethyloctyl group avoids the formation of braided chiral assemblies, thereby allowing molecules to organize into a cholesteric stack upon thermal annealing without encountering crystallization. These computational results are instrumental in the elucidation of the observed circular dichroism and circularly polarized fluorescence from neat films.

IV. Experimental Section

Materials Synthesis. All chemicals, reagents, and solvents were used as received from commercial sources without further purification except tetrahydrofuran (THF) and toluene that had been distilled over sodium/benzophenone and sodium, respectively. Intermediates **1**, **3**, and **23** as well as poly[9,9-bis(2*S*-methylbutyl)fluorene] were synthesized following a literature procedure.[14] Described below are the synthesis and purification procedures for the higher oligofluorenes, while those for the intermediates and **F(5*S*)-n** with n = 2−6 are included in the Supporting Information.

Hepta[9,9-bis(2*S*-methylbutyl)fluorene] (F(5*S*)-7). Into a mixture of **10** (0.200 g, 0.171 mmol), **14** (0.236 g, 0.360 mmol), and $Pd(PPh_3)_4$ (5 mg, 4.30×10^{-3} mmol) in a 50 mL Schlenk tube were added toluene (5 mL) and 2.0 M Na_2CO_3 solution (3.0 mL, 6.0 mmol). The reaction mixture was stirred at 90 °C for 2 days. After the mixture was cooled to room temperature, methylene chloride (50 mL) was added. The organic layer was separated and washed with brine for drying over $MgSO_4$. Upon evaporating off the solvent, the residue was purified with column chromatography on silica gel with petroleum ether: methylene chloride (5:1) as the eluent to yield **F(5*S*)-7** (0.176 g, 48%) as a white powder. ^{1}H NMR (400 MHz, $CDCl_3$): δ (ppm) 7.84−7.88 (m, 10H), 7.82 (d, J = 8.47 Hz, 2H), 7.77 (d, J = 7.28 Hz, 2H), 7.64−7.70 (m, 24H), 7.30−7.44 (m, 6H), 2.16−2.32 (m, 14H), 1.88−2.03 (m, 14H), 0.61−1.07 (m, 84H), 0.38−0.41 (m, 30H), 0.30−0.34 (m, 12H). Anal. Calcd for $C_{161}H_{198}$: C, 90.65; H, 9.35. Found: C, 90.79; H, 9.74.

Nona[9,9-bis(2*S*-methylbutyl)fluorene] (F(5*S*)-9). The procedure for the synthesis of **F(5*S*)-7** was followed to prepare **F(5*S*)-9** from **10** and **16** as a white powder in a 39% yield. ^{1}H NMR (400 MHz, $CDCl_3$): δ (ppm) 7.83−7.88 (m, 14H), 7.81 (d, J = 8.50 Hz, 2H), 7.77 (d, J = 7.29 Hz, 2H), 7.64−7.70 (m, 32H), 7.29−7.44 (m, 6H), 2.17−2.32 (m, 18H), 1.92−2.02 (m, 18H), 0.63−1.04 (m, 108H), 0.38−0.41 (m, 42H), 0.30−0.34 (m, 12H). Anal. Calcd for $C_{207}H_{254}$: C, 90.66; H, 9.34. Found: C, 90.44; H, 9.70.

Undeca[9,9-bis(2*S*-methylbutyl)fluorene] (F(5*S*)-11). The procedure for the synthesis of **F(5*S*)-7** was followed to prepare **F(5*S*)-11** from **10** and **20** as a white powder in a 40% yield. ^{1}H NMR (400 MHz, $CDCl_3$): δ (ppm) 7.83−7.88 (m, 18H), 7.81 (d, J = 8.46 Hz, 2H), 7.77 (d, J = 7.32 Hz, 2H), 7.64−7.70 (m, 40H), 7.31−7.44 (m, 6H), 2.17−2.32 (m, 22H), 1.93−2.02 (m, 22H), 0.63−1.06 (m, 132H), 0.38−0.42 (m, 54H), 0.30−0.35 (m, 12H). Anal. Calcd for $C_{253}H_{310}$: C, 90.68; H, 9.32. Found: C, 90.63; H, 9.74.

Octa(9,9-bis[2*S*-methylbutyl)fluorene] (F(5*S*)-8). A mixture of bis(1,5-cyclooctadiene)nickel(0) (Ni(COD), 0.100 g, 0.364 mmol), 2,2′-bipyridine (0.057 g, 0.364 mmol), and cyclodiene (0.040 g, 0.364 mmol) in anhydrous DMF (2.0 mL) and toluene (2.0 mL) was stirred at 80 °C for 30 min. Compound **19** (0.400 g, 0.308 mmol) in toluene (6.0 mL) was added in one portion. The reaction mixture was stirred at 80 °C for 2 days. After the mixture was cooled to room temperature, chloroform (100 mL) and 2.0 M HCl (100 mL) were added. The mixture was thoroughly stirred until the organic phase was clear. The organic layer was separated and washed with brine for drying over $MgSO_4$. Upon evaporating off the solvent, the residue was recrystallized with hexane containing a small amount of chloroform. The solid was collected by filtration to yield **F(5*S*)-8** (0.310 g, 83%) as a white powder. ^{1}H NMR (400 MHz, $CDCl_3$): δ (ppm) 7.83−7.88 (m, 12H), 7.81 (d, J = 8.49 Hz, 2H), 7.77 (d, J = 7.30 Hz, 2H), 7.63−7.70 (m, 28H), 7.29−7.44 (m, 6H), 2.17−2.32 (m, 16H), 1.94−2.03 (m, 16H), 0.62−1.04 (m, 96H), 0.37−0.41 (m, 36H), 0.29−0.34 (m, 12H). Anal. Calcd for $C_{184}H_{226}$: C, 90.66; H, 9.34. Found: C, 90.78; H, 9.75.

Dodeca[9,9-bis(2*S*-methylbutyl)fluorene] (F(5*S*)-12). The procedure for the synthesis of **F(5*S*)-8** was followed to prepare **F(5*S*)-12** from **21** as a white powder in a 43% yield. ^{1}H NMR (400 MHz, $CDCl_3$): δ (ppm) 7.83−7.88 (m, 20H), 7.82 (d, J = 8.40 Hz, 2H), 7.77 (d, J = 7.36 Hz, 2H), 7.63−7.71 (m, 44H), 7.30−7.44 (m, 6H), 2.17−2.33 (m, 24H), 1.94−2.03 (m, 24H), 0.63−1.06 (m, 144H), 0.36−0.42 (m, 60H), 0.30−0.35 (m, 12H). Anal. Calcd for $C_{276}H_{338}$: C, 90.68; H, 9.32. Found: C, 90.54; H, 9.33.

Hexadeca[9,9-bis(2*S*-methylbutyl)fluorene] (F(5*S*)-16). The procedure for the synthesis of **F(5*S*)-8**, except with 3 equiv of catalyst, was followed to prepare **F(5*S*)-16** from **22** as a white powder in a 61% yield. ^{1}H NMR (400 MHz, $CDCl_3$): δ (ppm) 7.83−7.88 (broad, 28H), 7.81 (d, J = 8.51 Hz, 2H), 7.77 (d, J = 7.31 Hz, 2H), 7.63−7.71 (m, 60H), 7.29−7.44 (m, 6H), 2.17−2.32 (m, 32H), 1.90−2.03 (m, 32H), 0.92−1.06 (m, 64H), 0.80 (broad, 32H), 0.63−0.72 (m, 96H), 0.37−0.42 (m, 84H), 0.29−0.34 (m, 12H). Anal. Calcd for $C_{368}H_{450}$: C, 90.69; H, 9.31. Found: C, 90.54; H, 9.33.

2,7-Bis[9,9-bis(3*S*,7-dimethyloctyl)-9′,9′,9″,9″,9‴,9‴-hexakis(2*S*-methylbutyl)-7,2′;7′,2″;7″,2‴-tetrafluoren-2-yl]-(9,9-bis(2*S*-methylbutyl)fluorene (F(5*S*)7F(10*S*)2). The procedure for the synthesis of **F(5*S*)-7** was followed to prepare **F(5*S*)7F(10*S*)2** from **27** and **16** as a white powder in a 30% yield. ^{1}H NMR (400 MHz, $CDCl_3$): δ (ppm) 7.84−7.88 (m, 14H), 7.82 (d, J = 8.47 Hz, 2H), 7.77 (d, J = 7.32 Hz, 2H), 7.64−7.72 (m, 32H), 7.29−7.44 (m, 6H), 1.97−2.33 (m, 36H), 1.42−1.47 (m, 4H), 0.63−1.3 (m, 156H), 0.38−0.42 (m, 30H), 0.30−0.34 (m, 12H). Anal. Calcd for $C_{227}H_{294}$: C, 90.20; H, 9.80. Found: C, 89.90; H, 9.61.

Molecular Structures, Morphology, and Thermal Transition Temperatures. ^{1}H NMR spectra were acquired in $CDCl_3$ with an Avance-400 spectrometer (400 MHz). Elemental analysis was carried out by Galbraith Laboratories, Inc. and Quantitative Technologies, Inc. A size exclusion chromatograph, equipped with a UV−vis absorbance detector, a 15° and 90° light-scattering detector, a differential viscometer, and a differential refractometer, as described previously,[15] was employed to determine the molecular weight distribution for **F(5*S*)-polymer**, from which the number- and weight-average molecular weights were calculated. The chemical purity of monodisperse oligofluorenes was further evaluated by size exclusion chromatography and high performance liquid chromatography (HPLC 1100 series, Agilent Technologies), as shown in the Supporting Information. Thermal transition temperatures were determined by DSC (Perkin-Elmer DSC-7) with a continuous N_2 purge at 20 mL/min. Samples were preheated to 370 °C followed by cooling at −20 °C/min to −30 °C before taking the reported second heating scans at 20 °C/min. Morphology and the nature of the phase transition were characterized with a polarizing optical microscope (DMLM, Leica, FP90 central processor and FP82 hot stage, Mettler Toledo).

Preparation and Optical Characterization of Neat Films. Optically flat fused silica substrates (25.4 mm diameter × 3 mm thick, transparent to 200 nm, Esco Products) were coated with a thin film of Nylon 66 and uniaxially rubbed. Approximately 100 nm thick, pristine films were prepared by spin casting from 1 wt % chloroform solutions on the treated substrates followed by drying in vacuo overnight. Films for electron diffraction (JEM 2000 EX, JEOL USA) were prepared following the same procedures except using single crystalline NaCl substrates (13 mm diameter × 2 mm thick, International Crystal Laboratories). These films were floated off in a trough filled with deionized water for mounting onto copper grids. Monodomain cholesteric films, 4 μm in thickness, were prepared by melting powdery samples between two fused silica substrates followed by thermal annealing for $^1/_2$ h before cooling to room temperature at a rate to avoid crystallization. Upon removing one of the substrates, the films were freeze-fractured in liquid nitrogen. Images of the cross section along the film normal were acquired with a scanning electron microscope (FESEM, LEO 982) for the determination of the cholesteric pitch.[44]

A UV−vis−NIR spectrophotometer (Lambda-900, Perkin-Elmer) was used to measure absorption spectra in dilute solutions and neat films. Circular dichroism spectra in dilute solutions and neat films were collected with a spectropolarimeter (J-710, JASCO). When the sensitivity range of this instrument was exceeded, the UV−vis−NIR spectrophotometer was outfitted with a combination of linear polarizers (HNP'B, Polaroid) and zero-order quarter waveplates (AO1521/4-355 and AO1521/4-425, Tower Optical Corp.) to produce a left- or right-handed circularly polarized beam. The difference in absorbance between the left- and right-handed circularly polarized incidents, $\Delta A = A_L - A_R$, was converted to ellipticity, θ, in millidegrees, using the following formula: $\theta = 32\,982 \cdot \Delta A$. Experimental artifacts[45] because of linear dichroism and linear birefringence were eliminated by averaging two measurements through rotation of the film by 90° around its normal. Fluorescence spectra were gathered on a spectrofluorimeter (Quanta Master C-60SE, Photon Technology International). The dilute solution spectra were taken with a 90° orientation between excitation and detection. In the case of solid films, a straight-through arrangement was adopted in which a liquid light guide (Photon Technology International) was used to direct the excitation at 370 nm onto the center of the film; the light guide also served as a polarization randomizer. It is noted that the reported spectra represent the average of two different fresh spots on each film. The optical setup for polarized fluorescence is as described previously.[46]

Variable angle spectroscopic ellipsometry is a nondestructive technique for the determination of the real, $n(\lambda)$, and imaginary part, $k(\lambda)$, of the complex refractive index, $n'(\lambda) = n(\lambda) + ik(\lambda)$, as well as the film thickness. For pristine films of **F(5*S*)-n** and the polymer analogue, reflection ellipsometry (V-VASE, J. A. Woollam Corp.) at 55, 60, 62, and 65° off the film normal and UV−vis spectrophotometry of unpolarized light at normal incidence were performed. The complex refractive index and film thickness from these films were extracted following literature procedures.[47,48] The procedures for extracting complex extraordinary and ordinary refractive indices, $n'_e(\lambda)$ and $n'_o(\lambda)$, and the film thickness for nematic and cholesteric films have also been reported[49a] on the basis of transmission ellipsometry and UV−vis spectrophotometry with linearly polarized light, both at normal incidence. In general, refractive indices and film thicknesses extracted from ellipsometry are accurate to within ±1% as shown by comparison to independent techniques;[49,50] our repeated measurements of refractive indices with ellipsometry have also demonstrated reproducibility to within ±1% of the mean. The orientational order parameter of a uniaxially aligned nematic film was also evaluated with UV−vis linear dichroism.

As the primary reference standard for fluorescence quantum yield (Φ_{PL}), 9,10-diphenylanthracene (DPA) (99%; Acros Organics) was repeatedly recrystallized from xylenes until pale yellow prism crystals were obtained. Anthracene (99%, Aldrich Chemical Co.) was recrystallized once from ethanol. Poly(methyl methacrylate) (PMMA, Polysciences) with a weight average molecular weight of 75 000 was used without further purification. About 5 μm thick PMMA films doped with 9,10-diphenylanthracene and anthracene at 10^{-2} M were spin-cast on fused silica substrates followed by drying in vacuo overnight. The low doping level was adopted to avoid concentration quenching which cannot be avoided in the case of the neat films. The film lightly doped with 9,10-diphenylanthracene was assigned a widely accepted value of 0.83.[51] The anthracene-containing film was characterized with the following formula:[51]

$$\frac{\Phi_{PL,s}}{\Phi_{PL,r}} = \frac{1 - 10^{-A_r}}{1 - 10^{-A_s}} \frac{B_s \overline{n_s^2}}{B_r \overline{n_r^2}} \tag{1}$$

where subscripts s and r refer to sample and reference, respectively, A denotes absorbance at the excitation wavelength, B is the integrated intensity across the entire emission spectrum, and $\overline{n^2}$ is defined as follows:

$$\overline{n^2} \equiv \frac{\int I(\lambda) n^2(\lambda) \mathrm{d}\lambda}{\int I(\lambda) \mathrm{d}\lambda} \tag{2}$$

in which $I(\lambda)$ stands for emission intensity, and the integration was performed over the entire spectrum. In all cases, n in the equation above was the average refractive index, $n(\lambda) = \sqrt{(n_e^2(\lambda) + 2n_o^2(\lambda))/3}$.[52] The fluorescence quantum yield was measured using the spectrofluorimeter described above with emission detected at 60° off-normal to prevent excitation light from entering the detector. The result for the anthracene-containing film, $\Phi_{PL} = 0.28 \pm 0.03$, agrees with the reported value of 0.27 in benzene and ethanol,[51] thus validating the experimental

(44) Bunning, T. J.; Vezie, D. L.; Lloyd, P. F.; Haaland, P. D.; Thomas, E. L.; Adams, W. W. *Liq. Cryst.* **1994**, *16*, 769.
(45) Rodger, A.; Nordén, B. *Circular Dichroism and Linear Dichroism*; Oxford University Press: Oxford, 1997.
(46) Katsis, D.; Kim, D. U.; Chen, H. P.; Rothberg, L. J.; Chen, S. H.; Tsutsui, T. *Chem. Mater.* **2001**, *13*, 643.
(47) Tammer, M.; Monkman, A. P. *Adv. Mater.* **2002**, *14*, 210.
(48) Ramsdale, C. M.; Greenham, N. C. *Adv. Mater.* **2002**, *14*, 212.
(49) (a) Schubert, M.; Rheinländer, B.; Cramer, C.; Schmiedel, H.; Woollam, J. A.; Herzinger, C. M.; Johs, B. *J. Opt. Soc. Am. A* **1996**, *13*, 1930. (b) Wu, S. T.; Warenghem, M.; Ismaili, M. *Opt. Eng.* **1993**, *32*, 1775.
(50) Wang, X. H.; Grell, M.; Lane, P. A.; Bradley, D. D. C. *Synth. Met.* **2001**, *119*, 535.
(51) Demas, J. N.; Crosby, G. A. *J. Phys. Chem.* **1971**, *75*, 991.
(52) Müller, W. U.; Stegemeyer, H. *Ber. Bunsen-Ges. Phys. Chem.* **1973**, *77*, 20.

procedure. In general, the presently reported Φ_{PL} values are accompanied by an uncertainty of ±10%.

Acknowledgment. The authors wish to thank L. J. Rothberg of the Department of Chemistry, and S. D. Jacobs and K. L. Marshall of the Laboratory for Laser Energetics, University of Rochester, for technical advice and helpful discussions. They also thank J. Elman and T. H. Mourey of Eastman Kodak Co. for assistance in ellipsometry and in the determination of the absolute molecular weight of a polyfluorene sample, respectively. The authors are grateful for the financial support provided by the National Science Foundation under Grant CTS-9818234, the Multidisciplinary University Research Initiative, administered by the Army Research Office, under DAAD19-01-1-0676, and the Defense University Research Instrumentation Program under DAAD19-00-1-0074. Additional funding was provided by the Department of Energy Office of Inertial Confinement Fusion under Cooperative Agreement No. DE-FC03-92SF19460 with the Laboratory for Laser Energetics and the New York State Energy Research and Development Authority. The support of DOE does not constitute an endorsement by DOE of the views expressed in this article.

Supporting Information Available: Synthesis and purification procedures, ^{1}H NMR spectral data, the results of elemental analysis for all of the intermediates and compounds **F(5*S*)-n** with n = 2−6, and chromatograms of HPLC and SEC of representative samples of **F(5*S*)-*n*** (PDF). This material is available free of charge via the Internet at http://pubs.acs.org.

JA026165K